Biol. Cybern. (2005) 92: 445–451
DOI 10.1007/s00422-005-0571-1

ORIGINAL PAPER

Biological Cybernetics

Petr Marsalek · Petr Lansky

Proposed mechanisms for coincidence detection in the auditory brainstem

Received: 28 October 2004 / Accepted: 18 March 2005 / Published online: 24 May 2004

Abstract Sound localization in mammals uses two distinct neural circuits, one for low- and one for high-frequency bands. Recent experiments call for revision of the theory explaining how the direction of incoming sound is calculated. We propose such a revised theory. Our theory is based on probabilistic spiking and probabilistic delay of spikes from both sides. We have applied the mechanism originally proposed as an operation on spike trains resulting in multiplication of firing rates. We have adapted this mechanism for the case of synchronous spike trains. The mechanism has to detect spikes from both sides within a short time window. Therefore, in both circuits neurons act as coincidence detectors. In the excitatory low-frequency circuit we call the mechanism the excitatory coincidence detection, to distinguish it from the mechanism of the inhibitory coincidence detection in the high-frequency circuit. The times to first spike and gains of the two mechanisms are calculated. We show how the output gains of the mechanisms predict the dip within the human frequency sensitivity range. This dip has been described in human psychophysical experiments.

List of symbols

D	Delay random variable
Δ	Coincidence detection window
T	Sound period
f	Sound frequency
δ	Maximum delay
$P(\Delta)$	Probability of coincidence detection
p	Probability of spike arrival

P. Marsalek (✉)
Charles University Prague, Department of Pathological Physiology,
U nemocnice 5, Praha 2, CZ-128 53, The Czech Republic
E-mail: marsalek@karlin.mff.cuni.cz
Tel.: +420-224-965-901
Fax.: +420-224-912-834

P. Marsalek · P. Lansky
Institute of Physiology, Academy of Sciences of the Czech Republic,
Vídeňská 1083, Praha 4, CZ-142 20, The Czech Republic
E-mail: lansky@biomed.cas.cz

1 Introduction

In sound localization interaural clues are used. These are the interaural time delay, also studied as the phase difference, the interaural intensity delay, and the spectral distortion in the outer ear. These parameters of sound are encoded in spike trains and are processed in successive relays of the auditory pathway. The speed of processing and decoding the sound parameters into a meaningful signal of the direction of the sound source has vital importance for survival. In mammals, the direction of sound is computed in two brainstem branches of the auditory pathway. The medial superior olive (MSO) is the site for lower sound frequencies and in the lateral superior olive (LSO) higher sound frequencies are processed. Both the MSO and the LSO are the first nuclei in the sound localization pathway, which collect inputs from both sides. To achieve sufficient time precision in both systems, coincidence detection (CD) must be the spike generation mechanism (Carr and Friedman 1999; Batra et al. 1997).

Our description of CD is inspired by the older results obtained by Srinivasan and Bernard (1976), where CD implements multiplication of input firing rates. Their results assume asynchronous input spike trains. We have adapted their observations for synchronous input spike trains. Our proposed spike processing mechanisms use probabilistic spike delivery and random timing delay (random time of spike conduction). In the previous papers, in Marsalek et al. (1997) and also in the following three references, the random spike delay is termed timing jitter. In Marsalek (2001) we have shown that the spiking probability changes with sound frequency. In Marsalek and Kofranek (2004, 2005) we described the probability using a function with abrupt changes. In this paper we further present a smooth function in this context.

Experimentally observed synchronization precision in the MSO and the LSO is the highest spike precision ever described in mammalian central nervous systems (Oertel et al. 2000). When observing neuronal firing rise in response to sound in any relay of auditory pathway, toward higher sound frequencies, a limit (or critical) frequency is reached; it is the

maximal firing rate of individual neurons. Beyond this frequency some of the spikes phase locked to sound are missing, effectively lowering the input to output frequency transfer ratio. One of the results we present here is the output firing frequency of the studied mechanisms in dependence on the main sound frequency.

2 Models and theoretical results

2.1 Probability density of coincidence detection

As in Srinivasan and Bernard (1976), we denote input from one side A, from the other side B, and output C. Spikes on both sides are generated by sound in both cochleas and are then processed and propagated in neural pathways. The CD is realized when input spikes from both sides are closer in time than constant Δ.

We can assume that the timing of the two spike trains from the two sides is at first delayed only by the interaural time delay. Spike trains are relayed from the first neuron of the pathway to the second, from the second to the next, and so on. Due to this neuronal relaying, spikes are subject to a delay with a random component. We assume that the random delays on both sides are mutually independent and identically distributed random variables D with a maximal value of δ:

$$0 \le D \le \delta\,. \tag{1}$$

We assume that the length of the window for CD Δ is not longer than the maximum delay δ and that the delay δ is not bigger than the sound period T,

$$0 \le \Delta \le \delta \le T\,. \tag{2}$$

The output neuron emits the spike only when the two spikes from both sides meet in a time interval shorter than Δ, in other words when the two spike delays D_A and D_B are closer in time than Δ:

$$|D_\mathrm{A} - D_\mathrm{B}| \le \Delta\,. \tag{3}$$

We denote the probability of this event $P(\Delta)$. For $\Delta = 0$, it holds that $P(\Delta) = 0$. In the case of $\Delta = \delta$, $P(\Delta) = 1$, and $P(\Delta)$ monotonically increases with Δ, thus $P(\Delta)$ as a function of Δ is a cumulative distribution function. Under the condition that D are distributed in accordance with a given probability density function $f(x)$, then $P(\Delta) = \mathrm{Prob}(|D_\mathrm{A} - D_\mathrm{B}| \le \Delta)$ can be calculated. The output spike is emitted at the moment of the latter input spike. We calculated the values of $P(\Delta)$ for specific examples of D and $f(x)$. We do not show them following the reviewer's advice. They are available upon request.

2.2 Excitatory coincidence detection (ECD)

The symmetric case is considered in this article, this means that the spike from side A and the spike from side B arrive independently with the same probability of p in each sound cycle. The probability that simultaneously one spike arrives from one side and the other from the other side is p^2. Neuronal firing saturates, therefore p depends on sound frequency f. We assume that p attains its value as follows: below a certain constant, we call it limit frequency, f_L, all spikes propagate and $p = 1$, while above the limit frequency, $p = f_\mathrm{L}/f$ (Marsalek 2001). When using these two functions for the probability p, p as a function of f would not be smooth at the point where $f = f_\mathrm{L}$. To get a smooth function we can use the following expression of f:

$$p(f) = \frac{1}{1 + \exp((2f - 4f_\mathrm{L})/f_\mathrm{L})}\,. \tag{4}$$

This function based on the observations from Marsalek (2001) was fitted at the point where $p(f) = 0.5$. $p(f)$ for $f_\mathrm{L} = 750\,\mathrm{Hz}$ of the ECD in (4) and also $p(f)$ for $f_\mathrm{L} = 3\,\mathrm{kHz}$ of the inhibitory coincidence detection (ICD) in the following Eq. (7) are shown in Fig. 1.

The probability that the coincidence is detected within one sound cycle is $p^2 P(\Delta)$. We substitute into this expression p from (4). Then we multiply this expression by the sound frequency f to get the output firing rate. We set $P(\Delta) = 1$ and further multiply this expression by $1/4$ in order to normalize the result to obtain the maximal output frequency max $f_\mathrm{ECD} < 200\,\mathrm{Hz}$, which is within the firing range observed in experiments. We get the output firing frequency f_ECD (Fig. 2):

$$f_\mathrm{ECD} = \frac{f}{4\big(1 + \exp((2f - 4f_\mathrm{L})/f_\mathrm{L})\big)^2}\,. \tag{5}$$

The paradigm, how to generate spikes in the ECD mechanism is shown in Fig. 3 following the schematics in Srinivasan and Bernard (1976). In their paper they implemented the CD mechanism using the set of leaky integrator neuronal models with the time constant comparable to the magnitude of Δ.

2.3 Inhibitory coincidence detection

First we start with the description of the ICD algorithm and next we show the output frequency calculations. In the ECD mechanism it was not necessary to distinguish between the spikes with respect to the side since both inputs were excitatory. In the ICD mechanism the spikes in addition have to arrive in the correct sequence. The spikes of excitatory neurons (side A) presynaptic to the LSO have to arrive after the spikes of inhibitory neurons (side B), otherwise the output spike cannot be generated. Compared with the case of the ECD, in analogy to (3), the coincidence and the right succession of excitation after inhibition are detected only in the case, when

$$0 \le D_\mathrm{A} - D_\mathrm{B} \le \Delta\,. \tag{6}$$

The probabilities p and $P(\Delta)$ have the same meaning as in the case of the ECD. The difference is that in the ICD mechanism, spike ordering does matter and therefore for $\Delta = \delta$ is $P(\Delta) = 1/2$. In order to δ get the maximal frequency of the second mechanism normalized, to meet max $f_\mathrm{ICD} =$ max $f_\mathrm{ECD} < 200\,\mathrm{Hz}$, we multiply the expression for the ICD

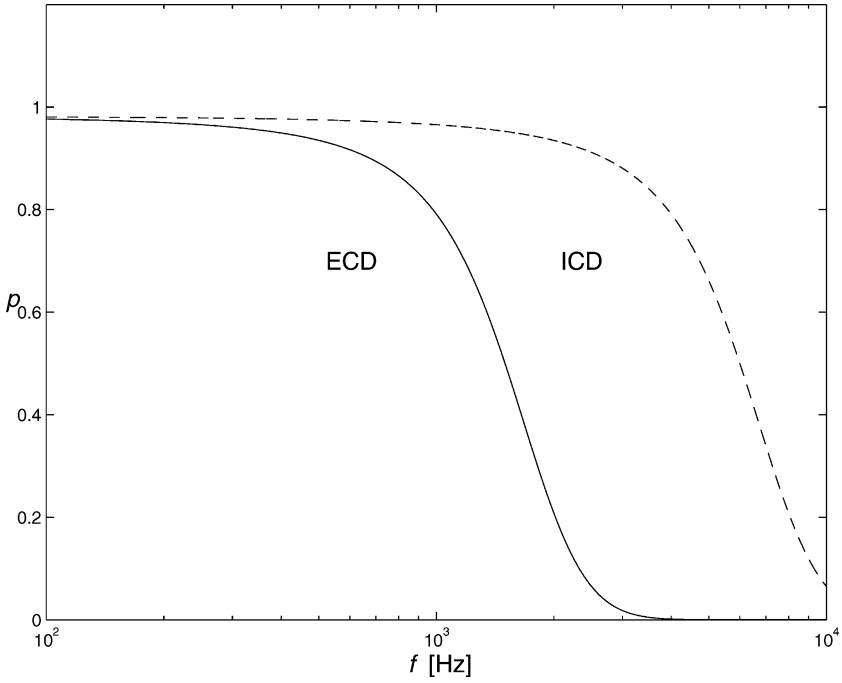

Fig. 1 Spike arrival probabilities. Probabilities p of spike delivery in dependency on main sound frequency f in logarithmic scale in Hz are shown here. The spikes constitute at both sides inputs into the MSO and LSO, to be processed by the ECD (*solid line*) and by the ICD (*dashed line*) mechanisms. The two functions are from the expression (4). *Solid* (ECD) and *dashed* (ICD) *lines* differ in the parameter f_{L}: $f_{\mathrm{L}} = 750\,\mathrm{Hz}$ for the ECD mechanism and $f_{\mathrm{L}} = 3\,\mathrm{kHz}$ for the ICD mechanism

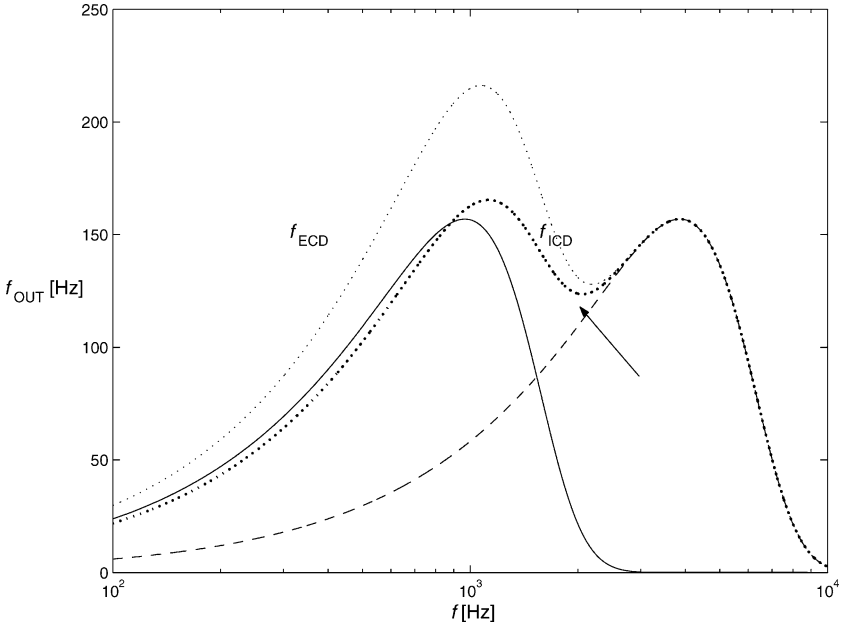

Fig. 2 Output frequencies in dependence on main sound frequency. The x-axis shows, in the logarithmic scale, main sound frequency f in Hz and on the y-axis there are output frequencies f_{OUT} in Hz of the ECD and of the ICD mechanisms, f_{ECD} and f_{ICD}. *Solid lines* show the ECD and dashed lines the ICD mechanisms, as in Fig. 1. The function for the ECD is in (5) and the function for the ICD is in (7). *Dotted lines, light and bold*, show how the two mechanisms can be pooled together to predict a psychophysical performance. The *light dotted line* is just the sum $f_{\mathrm{ECD}} + f_{\mathrm{ICD}}$. The *bold dotted line* shows the weighted sum of the two smooth functions with the ratio of 2:3, $(2/3)\,f_{\mathrm{ECD}} + f_{\mathrm{ICD}}$, which normalizes the sum of the two functions to keep the low-frequency part below 200 Hz and to preserve the high frequency part. The *arrow* shows the dip in the output firing frequency

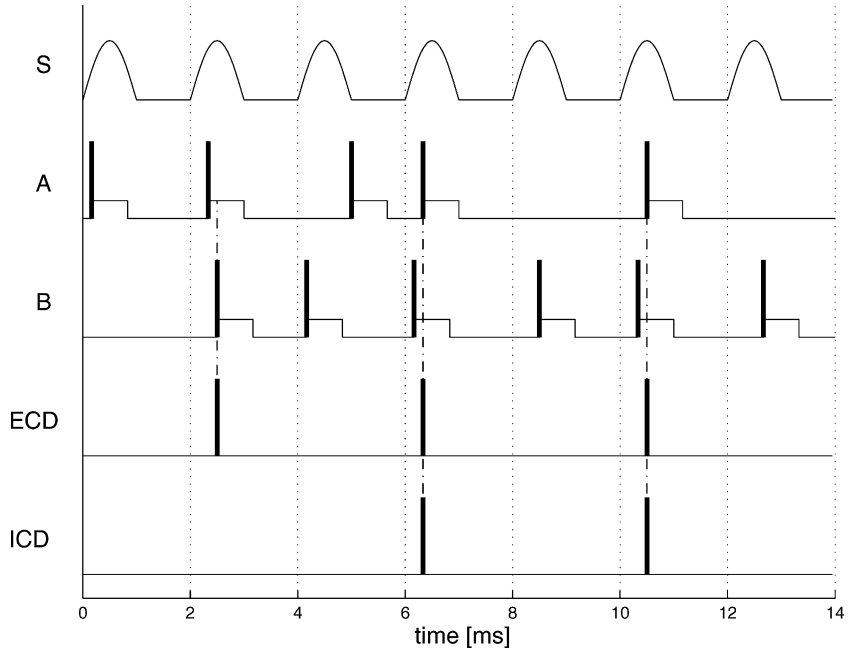

Fig. 3 The paradigm to determine the output spike train of the CD mechanisms. Spikes of neurons A and B follow leading edges of sound half-waves, top trace S, after random delays D_A and D_B. The windows of length Δ are triggered by the spikes. Bottom two traces: the spike train of the ECD is determined by placing the output spike aligned with the latter of the two spikes of A and B, if the two windows of length Δ overlap in time. For the output spike in the spike train of the ICD, all the conditions for the ECD are necessary and furthermore the (inhibitory) spike from side B must arrive sooner in time than the spike from side A. The window duration is $\Delta = 0.2$ ms, mean delays $E(D_A) = E(D_B) = 1$ ms. Proportions in the figure are schematic

by another factor equal to $1/8$. In summary, we multiply the expression (4) by $\frac{1}{8}p^2P(\Delta) = \frac{1}{16}p^2$ to get the function:

$$f_{\mathrm{ICD}} = \frac{f}{16\big(1+\exp((2f-4f_{\mathrm{L}})/f_{\mathrm{L}})\big)^2}\,, \tag{7}$$

which is analogous to the expression (5) for f_{ECD}.

2.4 The processing speeds of the ECD and of the ICD

A natural question to ask is, what is the typical processing time after the sound stimulus is turned on? This processing time will determine the processing speed and therefore the reaction time for the sound localization pathway as a whole. We have also calculated this processing time for the sake of comparison with other theories, presented in Discussion.

The procedure to calculate the processing time is shown in Fig. 4 for the values of $p = 0.35$ and 0.75. N is the number of sound cycles up to the cycle in which spikes at both neurons are generated together for the first time, N can take natural number values 1, 2, ... Let us denote $P(n)$ the probability that $N \leq n$. $P(n)$ is a cumulative distribution function of n. Using the spike delivery probability p, we calculate a probability, how many cycles it will take for the mechanisms of the ECD and of the ICD to generate their output. Let us characterize the processing time by two values: one is the number of cycles at which there is a 50% probability of generating the output spike, N_{50}, and the other value shows the number of cycles needed to reach a 95% probability that the output spike is generated, denote the latter N_{95}. The times to the first spike with given probabilities are at least $T_{50} = N_{50}T$ and $T_{95} = N_{95}T$, for the sound period T, because the delay D in the last sound cycle is not included in these simplified formulas. For simplicity we also set the coincidence detection probability in (3) to $P(\Delta) = 1$. The other cases, with $P(\Delta) < 1$, would be calculated analogously.

Let us find the minimal N_{50} such that the probability P of spike generation in cycle n is $P(n) > 0.5$. For this purpose we seek the minimal natural number N_{50} satisfying inequality:

$$1 - (1-p^2)^{N_{50}} \geq 0.5\,, \tag{8}$$

for unknown N_{50}. Analogously, in the 95% probability case, we seek the minimal natural N_{95} such that

$$1 - (1-p^2)^{N_{95}} \geq 0.95\,. \tag{9}$$

Solving these inequalities we get N_{50} and N_{95}.

The relevant frequency of the ECD mechanism ranges from 750 Hz to 3 kHz and p ranges from 1 to 0.25, respectively, using (5) with $f_{\mathrm{L}} = 750$ Hz. The frequency of the ICD mechanism ranges from 3 Hz to 12 kHz and p ranges from 1 to 0.25, respectively, using (7) with $f_{\mathrm{L}} = 3$ kHz. The estimated times to spike, not including the last D, will be $T_{50} = N_{50}T$ and $T_{95} = N_{95}T$. The times T_{50} and T_{95} are shown in Table 1.

Table 1 shows that in the ECD mechanism the waiting time gets longer toward higher frequencies. Therefore, there is an evolutionary pressure to develop some other mechanism for the higher frequency domain. The part showing results in

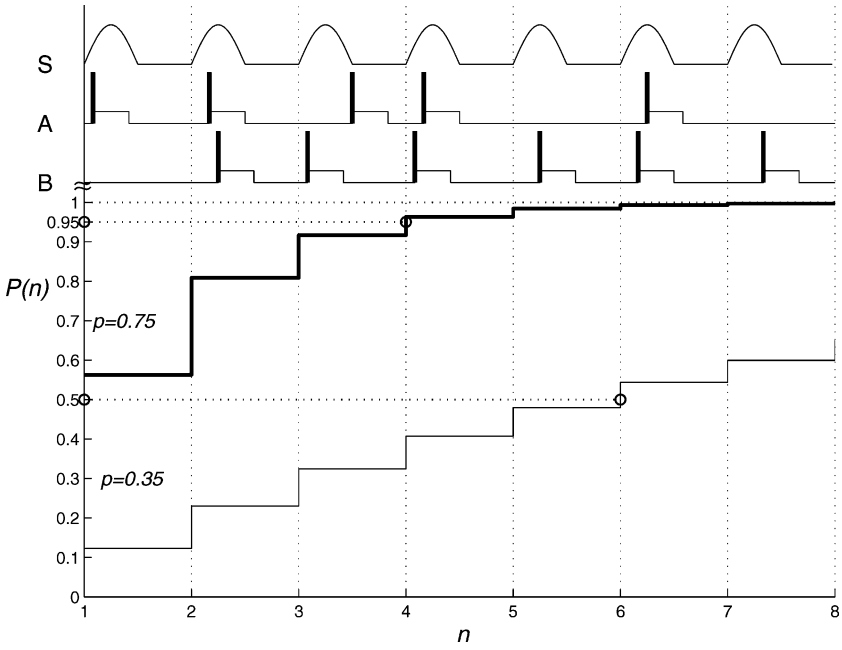

Fig. 4 Determining N_{50}, N_{95}, T_{50}, and T_{95} from $P(n)$. Top three traces are sound half-wave cycles S and example spike trains A and B. $P(n)$ is discrete and is discretized by the sound period steps. The values of $P(n)$ are as follows: during the first cycle it is $P(n) = p^2$, during the second cycle it is $P(n) = p^2 + (1 - p^2)p^2$, in the n-th cycle it is $P(n) = \sum_0^{n-1}(1 - p^2)^i p^2$ and these sums give the left sides in inequalities (8) and (9). $P(n) = 1$ for $n \to \infty$. Intersection of this staircase with horizontals at 0.5 and 0.95, respectively, gives the values of natural numbers N_{50} and N_{95}. Examples with $p = 0.35$, *light line*, and $p = 0.75$, *bold line*, are shown, the latter in order to demonstrate that N_{50} can even be equal to 1 for the value of $p > \sqrt{2}/2$

Table 1 The processing times of the ECD and of the ICD

f	ECD for various f (kHz)				ICD for various f (kHz)			
	750	1500	2.25	3	3	6	9	12
T_{50} in **ms**	1.33	2	2.67	3.67	0.33	0.5	0.67	0.92
T_{95} in **ms**	1.33	7.32	11.55	15.65	0.33	1.83	2.89	3.92

the ICD mechanism shows that the time to the first spike, signaling the approximate direction of the sound, is much shorter, compared to the mechanism of subtraction of firing rates, as we have shown in Marsalek and Kofranek (2005).

3 Discussion

This Discussion section contains a more detailed account of the experimental literature in order to review some of the experimental assumptions used in the model. It should also indicate which assumptions are not direct consequences of experimental observations. We start with the experiments on the MSO first. Next we proceed with the experiments on the LSO and also with the experiments on both the nuclei. Finally, we discuss the theoretical issues.

3.1 MSO experiments

Some of the current theories on the sound source localization mechanism in the MSO are still based on the classical theory of Jeffress (1948). Jeffress postulated the existence of the delay line as the mechanism for converting the microsecond time delays into the position within the array of neurons. The search for time delay sensitive neurons in the MSO and in the inferior colliculus of mammals motivated the experimental works of Goldberg and Brown (1969) and many others. Instead of finding an anatomically distinct delay line, a broad tuning of directional channels in the MSO was described around the year 2000 in various mammals, for example, in the guinea pig (McAlpine et al. 2001) and in the Mongolian gerbil (Brand et al. 2002). The importance of precise inhibition in the MSO was emphasized in Brand et al. (2002) and Svirskis et al. (2003). The experimental and modeling results of Brand et al. (2002) support the notion that no delay line is wired in the circuitry of the mammalian MSO. Our paper is also based on this notion.

3.2 LSO experiments and experiments on the whole superior olivary complex

A review of the theory on the subtraction of firing rates in the LSO can be found in (Tollin 2003). Neuronal responses in the LSO were investigated in fair detail in Joris and Yin (1995);

Joris (1996); Joris and Yin (1998). Following the experimental works on the MSO and those of Joris, we claim that the broadly tuned channels in higher frequency band are also present in the LSO. Batra et al. (1997) compared recordings from both the MSO and LSO and concluded that neurons in these two nuclei are endowed with two analogous spike generating mechanisms, based on the CD detection. Also Joris (1996) compares responses in the MSO and in the LSO. Firing rates of the responses fall into the range of 100–200 spikes per second. Therefore, we model the outputs as normalized to some value in both the MSO and the LSO to be < 200 Hz.

The novelty in our approach is in that we claim that the synchrony is used in the LSO. First, the anatomy around the MNTB neurons (neurons of the medial nucleus of trapezoid body which constitute the inhibitory input to the LSO) and the LSO neurons (neurons in both these nuclei are composed of thick fibers) indicates that timing is used, contrary to the current opinion. Second, there are also various data from experiments in cat: Oertel et al. (2000) obtain jitter less than 200 μs, with the 8 μs measurement bins in cochlear nuclei sending their axons into the LSO circuitry and Joris and Yin 1998 in the LSO itself show the vector strength higher than 0.5, which implies high synchronization accuracy, in a protocol where the interaural level difference is higher than 20 dB for all carrier frequencies up to 30 kHz. From these data it seems that Δ size in the LSO cells can be in the microsecond range and could be used, as we propose.

What remains unknown in current experiments, and could be measured by experimentation, is the average processing time estimated by the number of sound cycles, shown in Table 1. It is plausible that just a few sound cycles might constitute the putative processing time length in reality. This is also based on the observation by Joris and Yin (1998) of the conduction delay in the LSO circuitry: the contra-lateral (inhibitory) spike enters the LSO from 200 μs to 300 μs later than the ipsi-lateral (excitatory) spike. This corresponds to the length T of a sound cycle of frequency from 3.3 kHz to 5 kHz. This would imply that the contra-lateral input is one to two sound cycles later for the given sound frequencies. If the delays are as in this case the mechanisms for the particular characteristic frequencies should be discussed in the theory again from this perspective, as was also suggested by Batra et al. (1997).

We also conclude that the mechanism of subtraction of firing rates, which is a current prevailing explanation of the LSO spike processing, is too slow to be used in a real brainstem. When the first spike is generated according to the ICD paradigm in the LSO this first spike signals whether sound comes from the left or from the right hemisphere of sound space. The following spikes refine the spatial information, which gets more focused after each spike. After a sufficient amount of output spikes is accumulated, the LSO output will be indistinguishable on the longer time scale from the result of the firing rates subtraction. The concept of the ICD is also consistent with the same notion of the existence of two broadly tuned spatial channels in the LSO, which was originally formulated for the MSO responses.

The ICD mechanism gives its output faster than the subtraction of firing rates. An experiment deciding which of the two mechanisms is used in mammals, perhaps even in human subjects, can be designed as follows: within an artificial binaural stimulus, sound cycles should be deleted once randomly and once in alternating sound cycles or their multiples, and also incorporating one to two sound cycles lag of the contra-lateral side. This should modify the processing times predicted in Table 1 by not allowing for the coincidences crucial for the ICD mechanism.

3.3 Theoretical issues

Our previous description of coincidence detectors in single units in Marsalek (2000) was based on the data from detailed ion channel biophysics in the sound localization neurons from chicken brainstem slices, (Reyes et al. 1994, 1996), in models of Agmon-Snir et al. (1998) and in combined experimental and theoretical approaches, as in (Svirskis et al. 2003) and Szalisznyó and Zalányi (2004). Papers Brand et al. (2002) and Svirskis et al. (2003) compare experimental data with the deterministic Hodgkin–Huxley type models. Our paper studies these phenomena with the use of stochastic modeling of spike trains, triggered by a periodic input function. For a review on the theory of periodic input to stochastic models see Lansky (1997).

Kempter et al. (1998) searched for the range of time constants and the optimal number of excitatory postsynaptic potentials as steps to the threshold in an abstract neuron, as the parameters required for a neuron acting as a coincidence detector. According to Reyes et al. (1996) the number of incoming post-synaptic potentials in chicken binaural neurons is relatively low and gets progressively lower toward the higher sound frequencies due to the drop off above the limit frequency f_{L}. This can be expressed using probabilities. We adopted the approach of expressing it as probability, therefore we use the value of $p < 1$ as shown in Fig. 1. This imposes a ceiling for the rate values at lower sound frequencies, yet this can be also obtained by using a maximal rate and normalizing it to one. On the other hand, other authors, like Batra et al. (1997), argue that complex tuning curves observed in experiments can only be obtained by combining at least three inputs of different neuronal origin in first binaural neurons.

The dip in the directional sensitivity around the frequency of 1.5 kHz was described in psychophysical experiments in Mills (1972). When developing the model, we proceeded by deriving the formulas from the probabilities p dependent on f in Fig. 1 to the sensitivity data in Fig. 2. A possible experiment can proceed in the reverse order: from the dip in the sensitivity data, parameters of the model can be derived to achieve the closest fit to the sensitivity data. A basic parameter used in Fig. 1 is the limit firing frequency f_{L} in the ECD and its multiple in the ICD. This parameter has been used in a similar context in modeling before, for example, in Kral and Majernik (1996). The extrapolation of neuronal output to psychophysics requires the concept of population coding – the

outputs of the LSO and the MSO neurons have to be pooled to get the psychophysical performance. How exactly are they to be pooled is of course unknown and not accessible to experiment. Therefore, we suggest in Fig. 2 two simple plots to get the idea: light dotted line for pooling as $f_{ECD} + f_{ICD}$ and bold dotted line for pooling as $(2/3)\, f_{ECD} + f_{ICD}$.

A longer duration of Δ for spikes to be detected as coincident was suggested in Gerstner et al. (1996) as a possible mechanism of coincidence detection in other nuclei, especially in the neocortex. The parameters, which influence the time variance of random delay propagation to a higher nuclei along the pathway (termed "jitter" in Marsalek et al. (1997)) were further investigated by Reed et al. (2002), also in relation to the coincidence detection window size Δ.

Multiplication of spikes originally proposed by Srinivasan and Bernard (1976) and other alternative neuronal spike processing mechanisms are also discussed in Bugmann (1992). Srinivasan and Bernard (1976) were criticized that their "multiplicative" mechanism is too slow to be ecologically relevant. They argue against this criticism that the faster processing time can be achieved in population coding of the output rate by many neurons. In our, synchronous, case we do not face the objection that the waiting time for the output of multiplication is long, because there is some probability of an output spike with every sound cycle. However, the use of a population of binaural neurons will make the processing times even faster then the times shown in Table 1. In accordance with the discussion in Srinivasan and Bernard (1976) we do not claim that the sound location information is based on one cell output. This would actually result in quite poor performance for higher frequencies. Namely the question, how many cells should act together to get the processing times comparable for both low and high frequencies to reaction times would be a good question to investigate in some future theoretical study.

Acknowledgements This work was supported by the Academy of Sciences of the Czech Republic Grant, "Information Society", registration number: 1ET400110401, to Petr L., and by the Grant Research Initiative of the Ministry of Education, "Physiome.cz", registration number: 111100008 to Petr M. Thanks to Nick Dorrell.

References

Agmon-Snir H, Carr CE, Rinzel J (1998) The role of dendrites in auditory coincidence detection. Nature 393:268–272

Batra R, Kuwada S, Fitzpatrick DC (1997) Sensitivity to interaural temporal disparities of low- and high- frequency neurons in the superior olivary complex. I. Heterogeneity of responses. J Neurophysiol 78:1222–1236. II. Coincidence detection. J Neurophysiol 78:1237–1247

Brand A, Behrend O, Marquardt T, McAlpine D, Grothe B (2002) Precise inhibition is essential for microsecond interaural time difference coding. Nature 417:543–547

Bugmann G (1992) Multiplying with neurons: Compensation for irregular spike trains by using time-dependent synaptic efficiencies. Biol Cybern 68:87–92

Carr CE, Friedman MA (1999) Evolution of time coding systems. Neural Comput 11:1–20

Gerstner W, Kempter R, van Hemmen JL, Wagner H (1996) A neuronal learning rule for sub-millisecond temporal coding. Nature 383:76–78

Goldberg JM, Brown PB (1969) Response of binaural neurons of dog superior olivary complex to dichotic tonal stimuli: Some physiological mechanisms of sound localization. J Neurophysiol 32:613–636

Jeffress LA (1948) A place theory of sound localization. J Comp Physiol Psychol 41:35–39

Joris PX (1996) Envelope coding in the lateral superior olive. II. Characteristic delays and comparison with the responses in the medial superior olive. J Neurophysiol 76(4):2137–2156

Joris PX, Yin TC (1995) Envelope coding in the lateral superior olive. I. Sensitivity to interaural time differences. J Neurophysiol 73(3):1043–1062

Joris PX, Yin TC (1998) Envelope coding in the lateral superior olive. III. Comparison with afferent pathways. J Neurophysiol 79(1):253–269

Kempter R, Gerstner W, van Hemmen JL (1998) How the threshold of a neuron determines its capacity for coincidence detection. Biosystems 48:105–112

Kral A, Majernik V (1996) Neural networks simulating the frequency discrimination of hearing for non-stationary short tone stimuli. Biol Cybern 74:359–366

Lansky P (1997) Sources of periodical force in noisy integrate-and-fire models of neuronal dynamics. Phys Rev E 55(2):2040–2043

Marsalek P (2000) Coincidence detection in the Hodgkin–Huxley equations. Biosystems 58:83–91

Marsalek P (2001) Neural code for sound localization at low frequencies. Neurocomputing 38-40:1443–1452

Marsalek P, Koch C, Maunsell J (1997) On the relationship between synaptic input and spike output jitter in individual neurons. Proc Natl Acad Sci USA 94:735–740

Marsalek P, Kofranek J (2004) Sound localization at high frequencies and across the frequency range. Neurocomputing 58-60:999–1006

Marsalek P, Kofranek J (2005) Spike encoding mechanisms in the sound localization pathway. Biosystems 79:191–198

McAlpine D, Jiang D, Palmer AR (2001) A neural code for low-frequency sound localization in mammals. Nat Neurosci 4(4):396–401

Mills AW (1972) Auditory localization. In: Tobias JV (ed) Foundations of modern auditory theory. Academic, New York, pp 303–348

Oertel D, Bal R, Gardner SM, Smith PH, Joris PX (2000) Detection of synchrony in the activity of auditory nerve fibers by octopus cells of the mammalian cochlear nucleus. Proc Natl Acad Sci USA 97:11773–11779

Reed MC, Blum JJ, Mitchell CC (2002) Precision of neural timing: effects of convergence and time-windowing. J Comput Neurosci 14:35–47

Reyes AD, Rubel EW, Spain WJ (1994) Membrane-properties underlying the firing of neurons in the avian cochlear nucleus. J Neurosci 14:5352–5364

Reyes AD, Rubel EW, Spain WJ (1996) In-vitro analysis of optimal stimuli for phase-locking and time-delayed modulation of firing in avian nucleus laminaris neurons. J Neurosci 16:993–1007

Srinivasan MV, Bernard GD (1976) A proposed mechanism for multiplication of neural signals. Biol Cybern 21:227–236

Svirskis G, Dodla R, Rinzel J (2003) Subthreshold outward currents enhance temporal integration in auditory neurons. Biol Cybern 89(5):333–340

Szalisznyó K, Zalányi L (2004) Role of hyperpolarization-activated conductances in the auditory brainstem. Neurocomput 58-60:401–407

Tollin DJ (2003) The lateral superior olive: a functional role in sound source localization. Neuroscientist 9(2):127–143